# Metal-Oxide Film Conversions Involving Large Anions

**S. Pretty[1], X. Zhang, D.W. Shoesmith, and J.C. Wren**
[1]*The University of Western Ontario, Chemistry Department, 1151 Richmond St., N6A 5B7, London, Ontario, Canada,*
*jcwren@uwo.ca*

## ABSTRACT

Silver is a potential material for trapping fission product radioiodines and has the potential to safely transport and release radioiodines used in biomedical applications. However, reaction of I- with Ag could be complicated by the presence of silver oxide films. The kinetics of the conversion of Ag2O on Ag substrates to AgX (X = I or Br) are being followed by exposing electrochemically oxidized surfaces, with a known amount of Ag2O, to solutions containing I- or Br-.

Results show that two conversion pathways are possible; (i) a direct chemical process; and (ii) a galvanically coupled process in which the cathodic reduction of Ag2O is coupled to the anodic oxidation of Ag to AgX. Scanning electron microscopy results also revealed a difference in crystal structure of AgX depending on the conversion pathway, with fine particles resulting from the chemical conversion, and larger, better defined crystals growing via galvanic coupling.

## 1.0 INTRODUCTION

The objective of my graduate research is to establish the mechanism and kinetics of reactions involving metal-oxides and large anions ($I^-$, $Br^-$, $S^{2-}$). While film growth on metals, involving anions of a size similar to $O^{2-}$, has been extensively studied,[2-6] film formation involving larger anions ($S^{2-}$, $I^-$, $Cl^-$, etc.) has been essentially ignored, despite its industrial importance.

The proposed research has a range of industrial applications; for example, immobilization and release of radioiodine that is used as a cancer diagnostic or therapeutic agent can be optimized. Other applications of this research pertain to the nuclear power industry, where one of the safety issues is volatility assessment of radioiodines in the containment building environment in the event of an accident. One of the main products of fission from uranium fuel is radioiodines. Previous research has shown that in the event of an accident a significant amount of iodine would be released from the reactor core into the containment building.[7-9] Most of the released iodine would likely be dissolved in the ubiquitous water in the containment building, however, conditions in the containment building would be highly oxidizing making it possible for a small fraction of the released iodine to be vaporized (as $I_2$ (g) or organic iodides). In one of the severe accident scenarios, silver, used in some control rods for neutron flux, is assumed to be released into the containment building, where it too would likely be in the oxidized form. Previous studies have shown that silver is effective at trapping iodine,[7-9] however, the reactivity of $I^-$ and $I_2$ with silver surfaces varies depending on the oxidation state of the silver:

$$Ag_2O + 2\,I^- + H_2O \rightarrow 2\,AgI + 2\,OH^- \qquad (1)$$

$$Ag_2O + I_2 + 2\,H^+ + 2\,e^- \rightarrow 2\,AgI + H_2O \qquad (2)$$

$$2\,Ag + I_2 \rightarrow 2\,AgI \qquad (3)$$

Therefore, to determine the volatility of iodine under changing post-accident containment conditions, we need to establish the mechanism and kinetics of the individual reaction(s) of iodine with silver. In the future we plan to look into the copper/sulphide and iron/sulphide interaction, as it is important in microbiologically-active systems, including water pipes, nuclear waste containers, and oil and gas pipes.

We are particularly interested in establishing a relationship between the redox potential for a metal/metal halide (or sulphide) couple and the kinetics of chemical/electrochemical transformations of surface oxide and/or halide films. For this reason, the metals and anions to be studied will include Ag and Cu, and Group 6 ($O^{2-}$, $S^{2-}$) and Group 7 ($Cl^-$, $Br^-$ and $I^-$) anions. Other members in our research group are exploring the effect of these anions on steels.

The difference between equilibrium potentials ($E^e$) for these metal/metal oxide and metal/metal halide systems varies; $\Delta E^e = (E^e)_{Ag2O/Ag} - (E^e)_{AgI/Ag}$ is large for Ag but progressively smaller for the Cu and Fe systems. Comparisons between the anions within a given group will provide insight on the effect of anion size on the film conversion, while comparisons between the Group 6 and 7 anions will provide insight on the effect of anion oxidation state. In addition, these anions, unlike $O^{2-}$, provide rich aqueous chemical speciation; for example, ($I^-$, $I_2$, $IO^-$, $IO_3^-$, etc.). Various conversion processes (e.g. $Ag_2O$ to AgI) can be envisaged, and the main pathway will vary depending on the chemical/electrochemical environments; for example, for the $Ag_2O$ to AgI conversion in iodide solution:

1. Chemical transformation not involving the base metal,
   $Ag_2O + 2 I^- + H_2O \rightarrow 2 AgI + 2 OH^-$

2. Anodic reaction with the base metal by defect or ion transport through the oxide:
   Anodic Reaction: $2 Ag + 2 I^- \rightarrow 2 AgI + 2 e^-$
   Cathodic Reaction: $2 H_2O + 2 e^- \rightarrow 2 OH^- + H_2$
   Net Reaction: $2 Ag + 2 I^- + 2 H_2O \rightarrow 2 AgI + 2 OH^- + H_2$

3. Galvanic coupling through the substrate metal:
   Cathodic Reaction: $Ag_2O + H_2O + 2 e^- \rightarrow 2 Ag + 2 OH^-$
   Anodic Reaction: $2 Ag + 2 I^- \rightarrow 2 AgI + 2 e^-$
   Net Reaction: $Ag_2O + 2 I^- + H_2O \rightarrow 2 AgI + 2 OH^-$

4. Oxide dissolution, followed by iodide precipitation from solution:
   $Ag_2O + H_2O \rightarrow 2 Ag^+ + 2 OH^-$
   $Ag^+ + I^- \rightarrow AgI$

Which reactions dominate is expected to depend on parameters such as $\Delta E^e$, oxide and iodide film morphologies and thickness, film compositions and crystallinities, cation and anion oxidation states, solution redox conditions, etc.

A complication is the pseudo steady state that exists between $I^-$ and $I_2$ in aqueous solution [11]

$$I^- \Leftrightarrow I_2 \qquad (4)$$

$$I_2 + H_2O \leftrightarrow HOI + I^- + H^+ \qquad (5)$$

$$I_2 + I^- \leftrightarrow I_3^- \qquad (6)$$

Equilibria 5 and 6 are achieved thermally, even in the absence of radiation. Also, the availability of aqueous iodine species, mainly $I^-$ and $I_2$, would vary depending on radiation dose rate, pH, temperature, and the presence of impurities.[11]

The conversion pathways are expected to have an influence on the properties of the surface film formed, an important factor controlling corrosion kinetics. Thus, if we can establish how the dominant conversion pathway changes with respect to the chemical/electrochemical environment, the information can be used for corrosion control.

In my study, the surface reaction kinetics of the $Ag_2O$ to AgI conversion in aqueous iodide solutions was followed electrochemically.[10] We used a number of both electrochemical and surface analysis techniques to study the surface reaction kinetics, including: cathodic stripping voltammetry, galvanostatic reduction, voltammetry, electrochemical impedance spectroscopy. The electrochemical analysis techniques are augmented by surface analysis such as, scanning electron microscopy, energy dispersive X-ray spectroscopy, and in-situ Raman spectroscopy. Electrochemical techniques are extremely sensitive to changes occurring on the electrode surface. By combining electrochemical and surface analyses, we obtained a more detailed and complete understanding of the processes that occur at the electrode surface. These techniques are discussed in more detail later.

The conversion kinetics of $Ag_2O$ to AgI in aqueous iodide solutions at pH 12 was followed by electrochemically growing a known amount of silver oxide on Ag in iodide-free solution, and subsequently following the reaction in an iodide-containing solution on open circuit. The amounts of oxide and iodide on the Ag surface were determined at various reaction times, using cathodic stripping voltammetry (see Figure1). Complete conversion was indicated by an abrupt transition in the open circuit potential from a value close to the equilibrium potential for $Ag_2O/Ag$, $(E^e)_{Ag2O/Ag}$, to a value close to the equilibrium potential for AgI/Ag, $(E^e)_{AgI/Ag}$. This abrupt change in the open circuit potential allowed an easy determination of the total reaction time, $\tau_f$, required for complete conversion of $Ag_2O$ to AgI. The total reaction time as a function of iodide concentration and initial $Ag_2O$ inventory, and the amounts of AgI and $Ag_2O$ as a function of reaction time, t, determined by cathodic stripping voltammetry, were used to extract rate parameters for the chemical conversion. The rate was found to be first order in both iodide concentration and oxide surface area.

A second kinetic analysis has also been completed for the AgBr system and preliminary results reveal that, compared to the $Ag_2O$ and AgI system: (1) dissolution of AgBr is more significant, (2) the overall conversion of $Ag_2O$ to AgBr is slower than the conversion to AgI, and (3) the contribution of galvanic coupling through the silver metal to the overall conversion is more significant.

## 1 EXPERIMENTAL

### 1.1 Electrochemical cell and electrodes

A three-electrode system, consisting of a Ag working electrode, a Pt counter electrode, and a SCE reference electrode was used for all experiments, potential measurements are quoted against the SCE [+241 mV vs standard hydrogen electrode (SHE)]. The working electrode was a 7 mm diameter (surface area is 0.385 $cm^2$) Ag disk set in poly(tetrafluoroethylene) (PTFE) holders using epoxy resin so that only the front face was exposed to solution. Prior to each experiment, the Ag electrode was manually polished with 800 and 1000 grit silicon carbide papers. The electrode was then washed with Millipore water (18.2 MΩ cm), ultrasonically cleaned in an acetone/methanol mixture, and finally washed again with de-ionized water prior to experiments. The counter electrode was a platinum mesh (18 $cm^2$). A Solatron model 1240 potentiostat was used to control and measure potentials. Corrware and Corrview software (supplied by Scribner Associates) were used to control the potentiostat and analyze the data.

### 1.2 Solutions

All solutions were prepared using de-ionized Millipore water (18.2 MΩ cm). Solutions for electrode preoxidation were prepared with reagent-grade sodium hydroxide (97.0% assay) to a concentration of 0.01 M giving a pH of 12.0. Iodide solutions were prepared with reagent-grade potassium iodide (99.0% assay) in a concentration range of $4.0 \times 10^{-5}$ to $5.0 \times 10^{-3}$ M. Bromide solutions were prepared with reagent-grade potassium bromide (99.0% assay) in a concentration range of $5.0 \times 10^{-4}$ to $3.0 \times 10^{-3}$ M.

### 1.3 Experimental Procedure

All experiments were conducted at room temperature in Ar-purged 0.01 M NaOH (pH 12.0). A cathodic cleaning of the Ag electrode at a potential of – 1.1 V for 300s preceded all experiments. Cyclic voltammetric experiments were conducted from the cathodic cleaning potential to various anodic limits at a scan rate of 5 mV $s^{-1}$. After cathodic cleaning, a $Ag_2O$ film was grown potentiostatically by applying a potential of 0.4 V until the total oxidation charge reached a desired value, typically in the range of 0.05-0.2 C (0.013-0.52 C $cm^{-2}$). The pre-oxidized, $Ag_2O$-covered electrode was then transferred to a 0.01 M NaOH solution containing KI or KBr. The reaction between $Ag_2O$ and $I^-$ or $Br^-$ was monitored by measuring the open-circuit potential ($E_{OC}$) as a function of time (see Fig. 1). The reaction was terminated at various reaction times by transferring the electrode back to the KI/KBr-free solution. The electrode potential was immediately scanned from $E_{OC}$ to –1.1 V and the currents for the reduction of reactant $Ag_2O$ and the reaction product, AgI or AgBr, were measured.

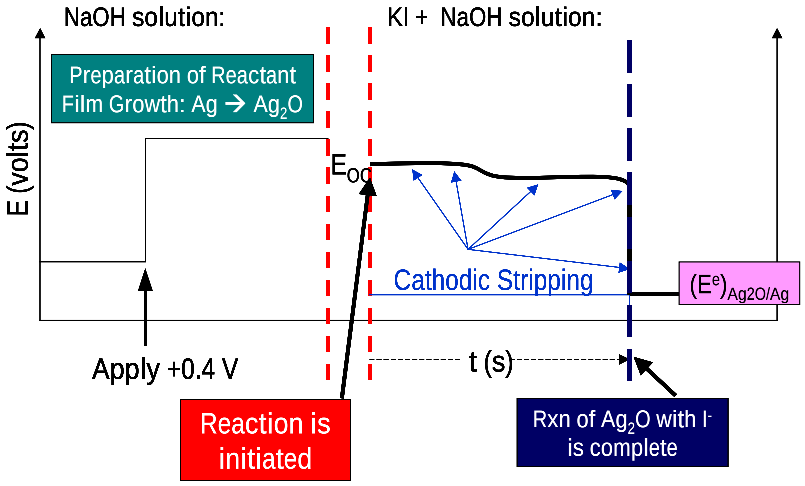

*Figure 1: A schematic of the general experimental procedure used to grow $Ag_2O$ films, follow the reaction with $I^-$ on open circuit, and determine the amounts of $Ag_2O$ and AgI as a function of reaction time.*

### 1.4 Surface Analytical methods

Raman spectroscopy was performed in-situ using a Renishaw model 2000 Raman Spectrometer, at a laser wavelength of 633 nm. Raman spectra were obtained periodically during the silver oxide to silver halide conversion process.

## 2 RESULTS & DISCUSSION

### 2.1.1 Overall Reaction Kinetics: Silver Oxide/ Silver Iodide System

The rate equation for the reaction of solid species $Ag_2O$ with aqueous species $I^-$ (via Reactions (1) and (3)) can be expressed as:

$$\frac{d(n_{AgI})_t}{dt} = -2\frac{d(n_{Ag2O})_t}{dt} = k(A_{Ag2O})_t^{\beta}[I^-]_t^{\alpha} \qquad \text{(Eq.1)}$$

where $(n_{Ag2O})_t$ and $(n_{AgI})_t$ are the number of moles of $Ag_2O$ and AgI at reaction time t; $[I^-]_t$ (in mol cm$^{-3}$) and $(A_{Ag2O})_t$ (in cm$^2$) are the concentration of $I^-$ and the surface area of $Ag_2O$ at time t; *k* is the reaction rate constant; and superscript, $\alpha$ and $\beta$, represents the reaction order with respect to $[I^-]$ and $(A_{Ag2O})$. The units of *k* will depend on $\alpha$ and $\beta$, and note that $[I^-]_t$ is in units of mol cm$^{-3}$, and the surface area is in cm$^2$. Also, we are assuming that *k* is the sum of the contributions from pathways (1) and (3). The goal then, is to establish values for *k*, $\alpha$, and $\beta$, but first I will describe how we used electrochemical methods to follow the chemical conversion of $Ag_2O$ to AgI.

### 2.1.2 Open Circuit Potential Behaviour as a Function of Time

The open circuit potential, $E_{OC}$, monitored during the chemical conversion of $Ag_2O$ to AgI, shows three distinct stages (Fig. 2). During Stage 1, $E_{OC}$ is close to $(E^e)_{Ag2O/Ag}$ of 0.22 V. For all cases studied, the initial $E_{OC}$ value was the same, regardless of the initial film thickness or $[I^-]$. The length of Stage 1 decreased with an increase in $[I^-]$ and a decrease in $(n_{Ag2O})_o$.

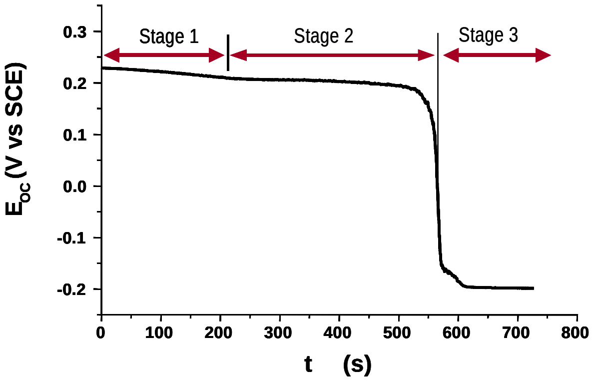

*Figure 2: Typical $E_{OC}$ behaviour of an $Ag_2O$ covered electrode in 0.01 M NaOH + $5.0 \times 10^{-4}$ M KI at pH 12.0.*

The chemical conversion of $Ag_2O$ to AgI continued for the duration of Stages 1 and 2, until all of the $Ag_2O$ was converted to AgI, as determined by measuring cathodic stripping voltammograms (see discussion below). A sudden drop in the potential marks the completion of the conversion, and the $E_{OC}$ in Stage 3 remains constant at a value slightly above the equilibrium potential for the reaction:

$$Ag + I^- \rightarrow AgI + e^-$$

The $(E^e)_{AgI/Ag}$ was calculated using the Nernst equation, and is dependent on $[I^-]$. The relationship between the final $E_{OC}$ (in Stage 3) and the $(E^e)_{AgI/Ag}$, strongly indicated that the Ag surface is fully exposed to the bulk $I^-$ solution, Fig. 3. The experimental and theoretical results are in close agreement. Cathodic stripping of the electrode performed immediately after the potential drop indicated the complete conversion of $Ag_2O$ to AgI. No presence of $Ag_2O$, and no further change in the amount of AgI as a function of duration of Stage 3, were observed. Therefore, once this final potential was reached, the chemical conversion was considered to be complete.

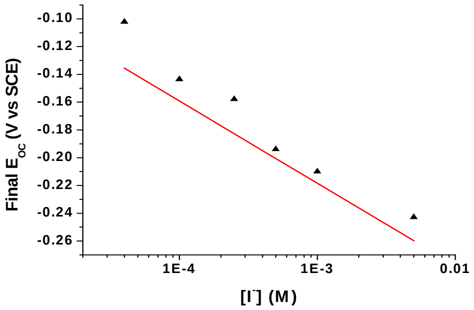

*Figure 3: Final steady-state open-circuit potential (symbols) observed for various $[I^-]$ compared to calculated equilibrium potentials for the $Ag + I^- \rightarrow AgI + e^-$ reaction (line).*

The $E_{OC}$ value during Stage 2 remained at ~0.2 V, and was attributed to a mixed potential of the redox reactions of silver-silver oxide and silver-silver iodide in iodide solution. If the surface iodide concentration was assumed to be the same as the iodide concentration in the bulk aqueous phase, the $E_{OC}$ corresponds to a large overpotential for the oxidation of Ag to AgI, which would result in considerable anodic formation of AgI by galvanic coupling. Our cathodic stripping and corrosion measurements indicate that this is not the case. Instead we interpret the decrease in $E_{OC}$ as a result of the lower concentration of $I^-$ at the electrode surface, which may be due to the fast reaction of $I^-$ with $Ag_2O$, preventing $I^-$ from reaching the metallic silver surface. The duration of Stage 2 also increased with an increase in $(n_{Ag2O})_o$ and a decrease in $[I^-]$.

In conclusion of the $E_{OC}$ measurements, the observed behaviour of the open circuit potential suggests that we can follow $E_{OC}$ to determine the total reaction time, $\tau_f$, easily. By measuring the total reaction time as a function of iodide concentration and initial $Ag_2O$ inventory, we can determine the rate parameters for the $Ag_2O$ to AgI conversion. The kinetic analysis using $\tau_f$ is presented later. The $E_{OC}$ values observed in Stage 2 also suggest that the galvanic coupling process (3) may be possible, requiring corrosion rate measurements.

### 2.1.3 Amounts of reactant $Ag_2O$ and product AgI as a function of reaction time

The overall conversion kinetics of $Ag_2O$ to AgI was followed by monitoring the extent of the reaction by electrochemical reduction of the reactant, $Ag_2O$ to Ag, and product AgI to Ag, as a function of reaction time.

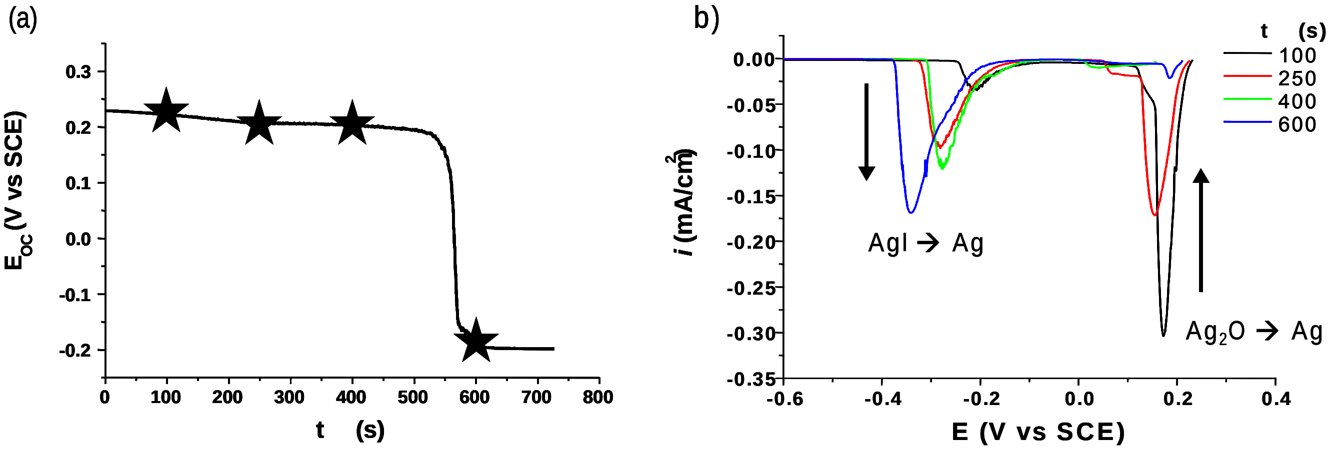

*Figure 4: CSV as a function of reaction time ($t_{rxn}$). The times when the CSVs were taken are indicated on the $E_{OC}$ plot in (a), and (b) the corresponding CSVs. The experimental conditions were 2 $(n_{Ag2O})_o$ = 4.6 x $10^{-7}$ moles, and $[I^-]$ = 5.0 x $10^{-4}$ M.*

Figure 4a shows the times during the open-circuit potential transient where the reaction was terminated, the electrode transferred to a KI-free solution, and a cathodic stripping voltammogram (CSV) recorded. The potential was scanned from $E_{OC}$ to –1.1 V at a scan rate of 0.17 $mVs^{-1}$. The slow scan rate was chosen in order to distinguish between the two distinct reduction peaks for $Ag_2O$ to Ag, and AgI to Ag. Due to the large difference in $(E^e)_{Ag2O/Ag}$ and $(E^e)_{AgI/Ag}$ the cathodic current peaks for the reduction of $Ag_2O$ to Ag and AgI to Ag are well separated.

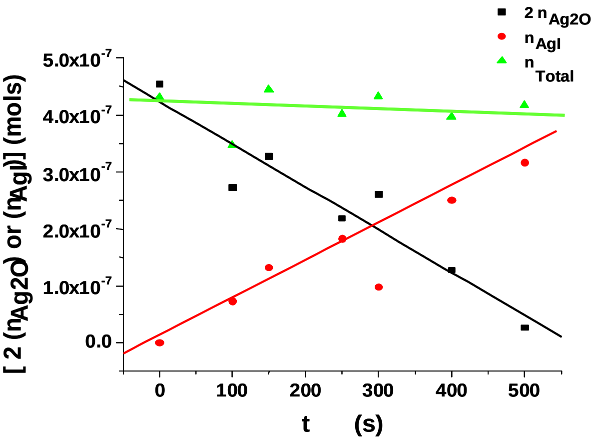

*Figure 5: Cathodic charges measured for the reduction of unreacted $Ag_2O$ and product AgI at various reaction times. The experimental conditions were $2\ (n_{Ag2O})_o = 4.6 \times 10^{-7}$ mols, and $[I^-] = 5.0 \times 10^{-4}\ mol\ dm^{-3}$.*

Integration of the two reduction peaks in Fig. 4b yielded values of $2\ (n_{Ag2O})_t$ and $(n_{AgI})_t$ as a function of reaction time. A plot of $2\ (n_{Ag2O})_t$ or $(n_{AgI})_t$ vs time (Fig. 6) reveals that throughout the reaction the following relationship exists:

$$n_{total} = 2\ (n_{Ag2O})_t + (n_{AgI})_t \cong 2\ (n_{Ag2O})_o \qquad \text{(Eq.2)}$$

The small decrease in $n_{total}$ with time indicates some dissolution of $Ag_2O$ over the reaction times. This confirmed that all of the anodic charge used to form the initial amount of $Ag_2O$ was retrieved when the remaining $Ag_2O$ and the product AgI were cathodically reduced. More importantly, the linear slopes reveal that the rate of loss of $2\ (n_{Ag2O})$, or production of $(n_{AgI})$, is constant with time. Since a surface reaction has a generalized rate law:

$$\frac{d\left(n_{AgI}\right)_t}{dt} = -2\frac{d\left(n_{Ag2O}\right)_t}{dt} = k\left(A_{Ag2O}\right)_t\left[I^-\right]_t^{\alpha} \qquad \text{(Eq. 3)}$$

the constant rate indicated that $[I^-]$ and $A_{Ag2O}$ are constant with time over the reaction. Since the initial amount of $Ag_2O$ was small and the electrode surface area to solution volume ratio is very small, the amount of $I^-$ reacted was also small. Thus $[I^-]_t$ should be constant and equal to $[I^-]_o$.

What was unusual for a surface reaction was that our results show a constant amount of $Ag_2O$ was exposed to $I^-$ during the reaction, i.e., $(A_{Ag2O})_t \approx (A_{Ag2O})_o$. The SEM micrographs of the electrode surface at various reaction times show that the chemically formed AgI (on open circuit) does not form a solid-state product, and suggests that the underlying layer of $Ag_2O$ is continuously exposed.

We then concluded that both $(A_{Ag2O})$ as well as $[I^-]$ do not vary significantly during the reaction for a given experimental condition, resulting in pseudo-zeroth order reaction kinetics. The reaction order dependence on the reactant concentration thus needs to be determined by changing the initial concentration of the reactant.

### 2.1.4 Reaction Order

The rate equation, under the conditions of $[I^-]_t \approx [I^-]_o$ and $(A_{Ag2O})_t \approx (A_{Ag2O})_o$, can be reduced to:

$$\frac{d(n_{AgI})_t}{dt} = -2\frac{d(n_{Ag2O})_t}{dt} = k(A_{Ag2O})_o [I^-]_o^{\alpha} \qquad \text{(Eq. 4)}$$

and its integration yields:

$$2\{(n_{Ag2O})_o - (n_{Ag2O})_t\} = (n_{AgI})_t = k\,(A_{Ag2O})_o [I^-]_o^{\alpha}\, t \qquad \text{(Eq. 5)}$$

At the total reaction time ($\tau_f$), when the conversion is complete, $(n_{Ag2O})_{\tau f} = 0$ or $(n_{AgI})_{\tau f} = 2\,(n_{Ag2O})_o$. Equation 7 at $\tau_f$ thus yields:

$$\tau_f = \frac{2(n_{Ag2O})_0}{k(A_{Ag2O})_0\,[I^-]_0} \qquad \text{(Eq. 6)}$$

or

$$ln\,\tau_f = ln\frac{2(n_{Ag2O})_0}{k(A_{Ag2O})_o} - \alpha\, ln\cdot[I^-]_0 \qquad \text{(Eq.7)}$$

Thus, for a given $Ag_2O$ film, and hence $(A_{Ag2O})_o$, the slope of the plot of log $[I^-]$ vs log $\tau_f$ (Fig. 6b) yields the reaction order, $\alpha$. The reaction rate dependence on $[I^-]$ was obtained from the total reaction time ($\tau_f$) as a function of $[I^-]_o$ for a given amount of 2 $(n_{Ag2O})_o$. The following experiments were conducted under the conditions where the initial amount of $Ag_2O$ was held constant at 2 $(n_{Ag2O})_o = 4.6 \times 10^{-7}$ moles, while the $[I^-]$ was varied from $4.0 \times 10^{-5}$ to $5.0 \times 10^{-3}$ M.

Figure 6(a) showed that as the initial concentration of $I^-$ increased, the final $E_{OC}$ (in Stage 3) decreased as the $(E^e)_{AgI/Ag}$ decreased with an increase in $[I^-]$ according to the Nernst equation.

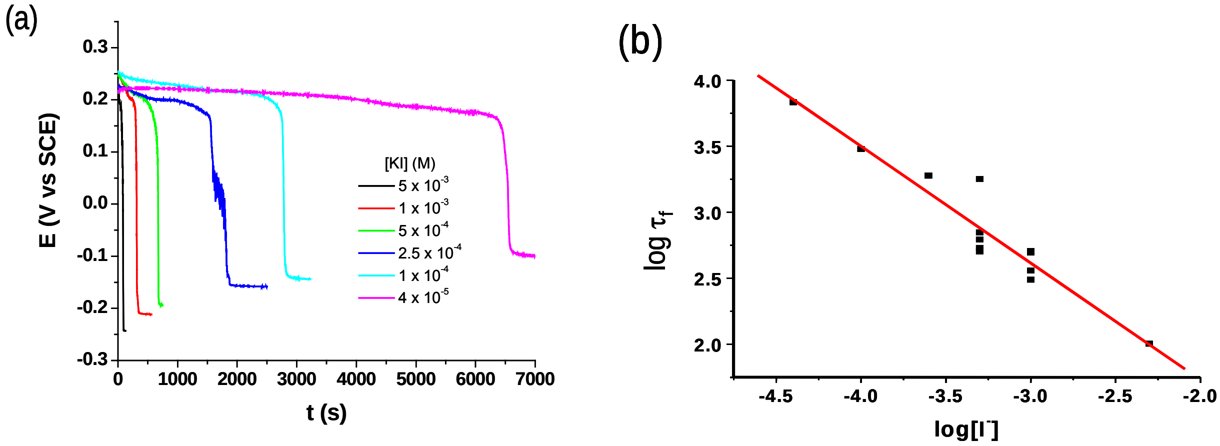

*Figure 6: (a) Open-circuit potential ($E_{OC}$) as a function of reaction time and its dependence on $[I^-]$. (b) Log of $[I^-]$ vs log of total reaction time, $\tau_f$.*

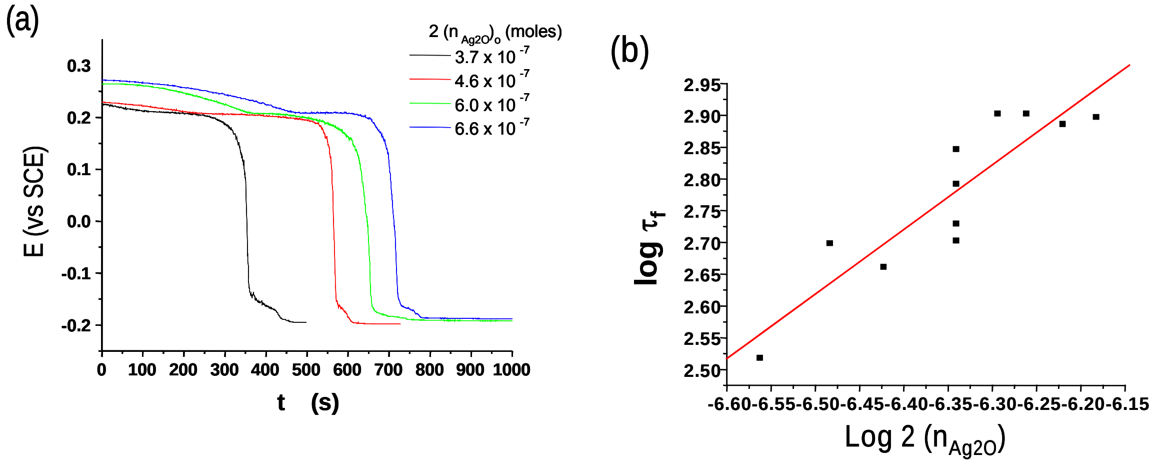

*Figure 7: (a) Open-circuit potential ($E_{OC}$) as a function of reaction time ($\tau_f$) and its dependence on 2 ($n_{Ag2O}$)$_O$. (b) Log of 2 ($n_{Ag2O}$)$_o$ vs log of total reaction time, $\tau_f$.*

We have also performed experiments in which the concentration of iodide was held constant at 5.0 x $10^{-4}$ mol dm$^{-3}$, while the 2 ($n_{Ag2O}$)$_o$ was varied from 3.7 x $10^{-7}$ to 6.6 x $10^{-7}$ moles, by applying +0.4 V for different times (Fig. 7). Equation 7 states that for a given $[I^-]_o$, the total reaction time will increase with an increase in the initial amount of 2 ($n_{Ag2O}$)$_o$. Since the total anodic charge, ($Q_{Ag2O}$)$_o$, used to grow the $Ag_2O$ film is proportional to 2 ($n_{Ag2O}$)$_o$, the plot of ln $\tau_f$ vs ln ($Q_{Ag2O}$)$_o$ should yield a slope of 1. Our experiments show a slope of ~0.90 (Fig. 8b). This slight deviation from a slope of 1 is attributed to the change in the surface area of $Ag_2O$, ($A_{Ag2O}$)$_o$, which varies slightly with the initial amount of $Ag_2O$ grown.

The $Ag_2O$ film was grown on a flat two-dimensional surface, however SEM micrographs of the $Ag_2O$ film show that the initial film growth does not occur uniformly, and the resulting surface is very bumpy and porous. Due to the uneven growth of three-dimensional $Ag_2O$ on the two-dimensional surface, we expect the surface area of the initial $Ag_2O$ film to have a small dependence on ($n_{Ag2o}$)$_o$. We have not yet determined the relationship between the initial amount of $Ag_2O$ and the initial area of $Ag_2O$, therefore for simplicity we assumed that the reaction is first-order in regards to ($A_{Ag2O}$)$_o$. Consequently, our kinetic analysis to date uses the geometric surface area, i.e. $A_{elec}$, of the Ag electrode (0.385 cm$^2$) and not the true $Ag_2O$ surface area.

### 2.1.5 Reaction Rate Constant

The integrated rate equation for the pseudo zeroth-order reaction yields:

$$\begin{aligned} 2\left(n_{Ag2O}\right)_t &= 2\left(n_{Ag2O}\right)_0 - k\left(A_{Ag2O}\right)_o\left[I^-\right]_0 t \\ &= 2\left(n_{Ag2O}\right)_0 - k_{app}A_{elec}\left[I^-\right]_0 t \end{aligned} \qquad \text{(Eq. 8)}$$

or

$$\begin{aligned} \left(n_{AgI}\right)_t &= k\left(A_{Ag2O}\right)_o\left[I^-\right]_0 t \\ &= k_{app}A_{elec}\left[I^-\right]_0 t \end{aligned} \qquad \text{(Eq. 9)}$$

Thus, from the slopes of the plot of 2 ($n_{Ag2O}$)$_t$ vs. t or ($n_{AgI}$)$_t$ vs. t obtained under a given condition, one can extract $k_{app}$. The slopes from Figure 5 yield $k_{app}$ = 3.1 x $10^{-3}$ cm s$^{-1}$. Although the analysis of the data obtained this way is straightforward, determination of $k_{app}$ using cathodic stripping voltammetry was, however, quite labour intensive as the electrode had to be rinsed and transferred to another cell to perform the CSV. This method also introduced a considerable amount of experimental uncertainty, as it is not known whether the reaction is completely terminated upon rinsing and transferring the electrode.

Alternatively, since the surface reaction has been shown to be a pseudo-zeroth reaction, the rate constant can be obtained from the total reaction time, which was easily determined from the open circuit potential measurements.

$$ln\,\tau_f = ln\frac{2\left(n_{Ag2O}\right)_0}{k\left(A_{Ag2O}\right)_o} - \alpha\, ln\cdot\left[I^-\right]_0 \qquad \text{(Eq.10)}$$

and the rate constant was 3.4 x $10^{-3}$ cm $s^{-1}$; this is in good agreement with the $k_{app}$ value obtained from the CSV measurements. The calculated $k_{app}$ values are also in agreement with the $k_{app}$ obtained for the conversion of $Ag_2O$ to AgI in 0.02 M $NaH_2PO_4$. For a more complete kinetic analysis see J. C. Wren, X. Zhang, S. Stewart and D.W. Shoesmith, *J. Electrochem. Soc.*, **154**, F70 (2007).

### 2.1.1 Overall Reaction Kinetics: Silver Oxide/ Silver Bromide System

Since the purpose of this research is to determine the effect of anion size and charge on metal oxide film conversions the same techniques were used to study the chemical conversion of $Ag_2O$ to AgBr. A partial kinetic analysis was completed for the AgBr system and preliminary results reveal: (1) the chemical conversion of $Ag_2O$ to AgBr is slower than the conversion to AgI due to the longer reaction time, (2) dissolution of AgBr was significant, and (3) galvanic coupling through the silver metal is significant. Some of these preliminary results are discussed in more detail below.

The $Br^-$ anion differs from the $I^-$ anion in a number of ways; firstly $Br^-$ is smaller than $I^-$ and the equilibrium potential for the Ag/AgBr system is much higher than that of the Ag/AgI system. Again, the $(E^e)_{AgBr/Ag}$ is dependent on the concentration of $Br^-$, and can be calculated using the Nernst equation, for $[Br^-]$ = 5.0 x $10^{-4}$ M the calculated $(E^e)_{AgBr/Ag}$ was 0.014 V.

The chemical conversion of $Ag_2O$ to AgBr was also possible through the same three reaction pathways discussed above in the $I^-$ case:

(1) Chemical $Ag_2O + 2\,Br^- + H_2O \rightarrow 2\,AgBr + 2\,OH^-$

(2) Electrochemical (Anodic Formation) $Ag + Br^- \rightarrow AgBr + e^-$

(3) Electrochemical (Galvanic Coupling) $Ag_2O + H_2O + 2\,e^- \rightarrow 2\,Ag + 2\,OH^-$
$2\,Ag + 2\,Br^- \rightarrow 2\,AgBr + 2\,e^-$

Net Reaction: $Ag_2O + 2\,Br^- + H_2O \rightarrow 2\,AgBr + 2\,OH^-$

Figure 8a shows the $E_{OC}$ as a function of reaction time for $[Br^-]$ ranging from 5.0 x $10^{-4}$ to 3.0 x $10^{-3}$ M. Like the iodide case, the final $E_{OC}$ was dependent on $[Br^-]$, and remained just above the calculated $(E^e)_{AgBr/Ag}$ values (Fig. 9b). The rate constant of the overall conversion of $Ag_2O$ to AgBr was calculated from the total reaction time as a function of $[Br^-]$, $k_{app}$ was determined to be 1.5 x $10^{-3}$ cm $s^{-1}$ which is ~ 2 times slower than the conversion in iodide solution. The calculated $k_{app}$ is a function of the contribution from both the chemical conversion pathway as well as the galvanic coupling conversion pathway.

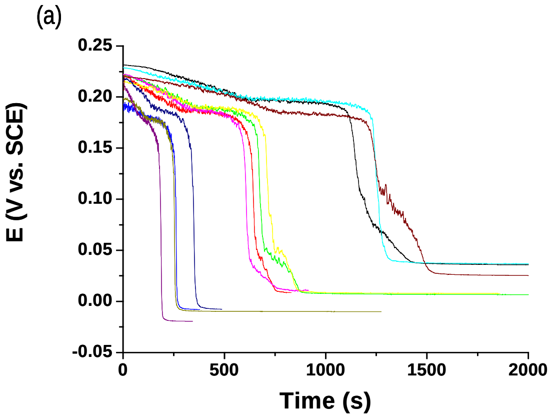

*Figure 8: Open-circuit potential ($E_{OC}$) as a function of reaction time and its dependence on [$Br^-$] (a). Final steady-state open-circuit potential (symbols) observed for various [$Br^-$] compared to calculated equilibrium potentials (b) for the Ag + $Br^-$ → AgBr + $e^-$ reaction (line).*

The initial $E_{OC}$ in bromide solution is lower than $(E^e)_{Ag2O/Ag}$, and the larger the bromide concentration, the lower the initial $E_{OC}$ (see Fig. 8a). This suggests that some bromide has diffused to the metallic Ag surface, most likely due to the slower reaction of $Br^-$ with $Ag_2O$ (as discussed above) and the faster diffusion rate of $Br^-$. At this high potential, there may be some anodic conversion of Ag to AgBr, and the galvanic coupling corrosion would have started already.

This corrosion rate is expected to be small in Stage 1 because $E_{OC}$ is not far from $(E^e)_{Ag2O/Ag}$ so the cathodic reaction should be very slow. So in Stage 1, the reduction of $Ag_2O$ to Ag limits the galvanic coupling rate.

The potential in Stage 2 is in fact nearly constant (both in iodide and bromide cases). In this stage, $I^-$ or $Br^-$ transport is likely the limiting step for the galvanic coupling process, and $E_{OC}$ may be determined by the diffusion rate of the anion. The large overpotential ($E_{OC}$ - $(E^e)_{AgI/Ag}$) required for iodide films is a further indication of slower transport of $I^-$, compared to $Br^-$. This may be due to a slower diffusion of $I^-$ in the aqueous phase as well as the faster reaction of $I^-$ with $Ag_2O$. Once the potential has reached Stage 3, no corrosion current was measured and no further formation of AgBr was observed. The maximum corrosion current was much lower in the $Br^-$ case compared to the $I^-$ case, however the corrosion current during the conversion of $Ag_2O$ to AgBr during Stages 1 and 2 is not negligible, and hence the net corrosion or net galvanic coupling is more significant in the $Br^-$ case.

Galvanostatic reduction at Stage 3 reveals there is no $Ag_2O$ present on the electrode surface, and dissolution of silver is significant and by Stage 3, about 50 % of the initial $Ag_2O$ was not retrieved. The amount of AgBr recovered during galvanostatic reduction should be equal to twice the initial amount of Ag2O. However, results show that as the reaction progressed, the amount of AgBr retrieved during galvanostatic reduction decreased. It is hypothesized that the slower reaction and higher solubility of AgBr with longer dissolution time for $Ag_2O$ account for the increase in dissolution of silver. Therefore, the cathodic stripping and galvanostatic reduction methods alone cannot be used for the kinetic analysis, but the galvanic coupling dissolution kinetics must be included. The dissolution kinetics will be examined in the near future.

## 3 CONCLUSIONS

The chemical conversion of $Ag_2O$ to AgI and AgBr in aqueous solutions was studied by following the open circuit potential as a function of time. An abrupt transition in the open-circuit potential from a value close to the $(E^e)_{Ag2O/Ag}$ to a value close to the $(E^e)_{AgI/Ag}/(E^e)_{AgBr/Ag}$ indicated the completion of the chemical conversion. The clear transition from $Ag_2O$ to AgX (X= $I^-$ or $Br^-$) allowed us to easily determine the total reaction time required for the chemical conversion to be complete. The total reaction time was inversely related to iodide/bromide concentration and directly proportional to the initial amount (or concentration) of $Ag_2O$.

The kinetic analysis established that the chemical reaction rate was first order in iodide concentration, and nearly first order in the initial amount of silver oxide. The rate of conversion, as determined by cathodic stripping voltammetry, was found to be constant. We attribute this to the fact that the product AgI did not form a protective layer on the $Ag_2O$ surface, therefore the effective surface area of $Ag_2O$ available for the reaction was constant.

The apparent rate constant was obtained from both the total reaction time measurements, which are based on the abrupt change in the open-circuit potential, as well as the cathodic stripping voltammetry measurements, which are based on the changes in the cathodic charges for $Ag_2O$ and AgI.

The partial kinetic analysis on the conversion of $Ag_2O$ to AgBr suggests that the difference in anion size may significantly change the conversion pathway, as galvanic coupling seems to play a major role in the bromide case. Initial open-circuit potential measurements indicate that some bromide may have diffused to the metallic Ag surface, which could lead to the electrochemical formation of AgBr via the galvanic coupling pathway. A full kinetic and corrosion study is planned to determine if in fact, galvanic coupling is more significant.

Based on the kinetic data obtained, rate equations were derived which can be used in models developed to predict the fate of radioiodine in various proposed nuclear reactor accident scenarios.

## 4 AKNOWLEDGEMENTS

This research was funded by a grant from the Natural Science and Engineering Council of Canada (NSERC) and a start-up grant from the Faculty of Science, at the University of Western Ontario. The electrochemical equipment was purchased from a grant from Canada Foundation for Innovation. Surface Science Western is thanked for the use of their SEM/EDX instrument.

## 8 REFERENCES

[1] Bard, A.J.; Faulkner,L.R. In *Electrochemical Methods: Fundamentals and Applications*; Harris, D., Swain, E., Robey, C., Aiello, E., Eds.; John Wiley & Sons: United States of America, 2001, p 99-104.

[2] M. Hepel and M. Tomkiewicz, *J. Electrochem. Soc.*, **131**, 1288 (1984).

[3] B.J. Murray, Q. Li, J.T. Newberg, E.J. Menke, J.C. Hemminger and R.M. Penner, *Nano Letters*, **5**, 2319 (2005).

[4] B.M. Jovic, V.D. Jovic and G.R. Stafford, *Electrochem. Commun.*, **1**, 247 (1999).

[5] J. Kunze, H.H. Strehblow and G. Staikov, *Electrochem. Commun.*, **6**, 132 (2004).

[6] T.U. Hur and W.S. Chung, *J. Electrochem. Soc.,* **152**, A179 (2005).

[7] J.C. Wren and J.M. Ball, *J. Rad. Phys. and Chem.*, **60**, 577 (2001).

[8] E. Krausmann and Y. Drossinos, *J. of Nucl. Materials*, **264**, 113 (1999).

[9] N. Girault, S. Dickinson, F. Funke, A. Auvinen, L. Herranz and E. Krausmann, *Nucl. Eng. and Design*, **236**, 1293-1308 (2006).

[10] J. C. Wren, X. Zhang, S. Stewart and D.W. Shoesmith, *J. Electrochem. Soc.*, **154**, F70 (2007).

[11] D. Jaquemain, N. Hanniet, C. Poletiko, S. Dickinson, C. Wren, D.A. Powers, E. Krausmann, F. Funke, R. Cripps, and B. Herrero, in *Proceedings of the OECD Workshop on Iodine Aspects of Severe Accident Management,* Vanata, Finland, 57 (1999).